International Journal of Current Engineering and Technology
E-ISSN 2277 – 4106, P-ISSN 2347 – 5161

Available at http://inpressco.com/category/ijcet

Research Article

Theoretical and Experimental study of the Behavior of Metals under Multi Axial Fatigue Failure

Fathi Abdul Sahib Alshamma and Mohammed Abdul Gani Gali*

Engineering College-Baghdad University, Iraq

Accepted 02 Feb 2017, Available online 11 Feb 2017, **Vol.7, No.1 (Feb 2017)**

Abstract

In this paper, a theoretical and experimental study of the behavior of metals under multiaxial fatigue by combination of cycling bending with torsion for non-proportional loading. In the theoretical analysis, Mohr circle have been used to get the principal stress in a test of multiaxial fatigue and inserted them in the von mises theory to get the suitable value of torsion with cycling bending stress. In the experimental part it was needed to manufacture multiaxial fatigue test machine to find the non-proportional fatigue properties of testing metals which have different mechanical behavior to identify the life of fatigue of metals and shape of the resulting fracture after exposing specimens to either reversed bending for verification the experimental results and combined bending with torsion stresses for L690M steel, C26800 brass, copper and 2117-T4 Aluminum in multi axial fatigue. The results show that when taking the stress ratio ($\lambda = \tau / \sigma_a$) constant for all metals used in this study, it was found that copper and 2117-T4 aluminum is the most resistant to multi axial fatigue failure, while C26800 brass, and L690M steel have less resistance It is clear from the surface fracture of the specimens' that multiaxial fatigue will effect on the orientation of maximum Shear stress and its values which inclined the crack evolution when compared with the axial fatigue

Keywords: *Multi Axial Fatigue Failure etc.*

1. Introduction

The purpose of the fatigue test device of metals is that for running the test fatigue metal and access to failure stage by the effect of cyclic loading on the specimen in one direction (uniaxial fatigue) which is usually rotating or reversed bending used for measuring the fatigue life of metals. **Ali Fatemi and Nima, S., 2011.**

There is a group of research, of which for **Bernasconi, S. and Foletti, I. V., 2005** study the effect of multiaxial fatigue on the metal type 39NiCrMo3 steel after exposure to axial-torsion fatigue tests two cases proportional and non-proportional loadings. The results appeared to crack growth speed and fatigue life, concluded that the test non proportional is more dangerous than proportional with survival of stress a constant value. Also paper for **Zbigniew Marciniak, et al., 2007** discusses the results of fatigue tests 10 HNAP and 18G2A steel under combined bending and torsion stresses for two cases proportional and non-proportional, and used circular smooth specimens. The tests were carried out in the fatigue test device stand "MZGS-200L". Experimentally show that the fatigue life under non-proportional loading for steel greater (up to 10 times) than under the proportional loading on the same value of normal and shear stresses. Also **Xiao-Yong Liu,et al., 2015** used samples of the two type's smooth specimen and notched specimen, this specimens exposed to multiaxial high cycle fatigue. Is calculated fatigue life by using Finite Element Method (FEM). Concluded that both types of samples in the case of multiaxial fatigue non-proportional loading less dangerous and longer fatigue life of the test case proportional loading with survival value von Misses stress amplitude constant.

Today it is needed to develop advice based on fatigue test in metal by more than one axial loading (multiaxial fatigue) by combined cyclic bending and torsion because a lot of parts have been failed by proportional and non proportional, multiaxial cycling loading for example very clear in the crankshaft, spline shafts, aircraft wing and other mechanical parts**, K. J. Miller and M. W. Brown, 1999.**

The purpose of this study is to Study the effect of the multiaxial (bending with torsion fatigue) on the value and orientation of the max shear stress for metals (L690M steel, C26800 brass, copper and 2117-T4 Aluminum) which effect on the direction of the crack propagation and the number of cycles to failure.

2. Theoretical Analysis

In the first step of calculation it must be known the value of the shear stress that can be applied to the

*Corresponding author **Mohammed Abdul Gani Gali** is a Researcher and **Dr. Fathi Abdul Sahib Alshamma** is working as Assistant Professor

specimen as a cantilever beam subjected to combined bending and torsion without exceeding the elastic limit.so the shear stress could be calculated as follow :-

$\tau_{xy} = \frac{\theta * G * r}{l}$ Let $(c=\frac{G*r}{l})$

$$\tau_{xy}(\theta) = c * \theta \quad (1)$$

$$\sigma_{1,2} = -\left(\frac{\sigma_x+\sigma_y}{2}\right) + \frac{1}{2}[(\sigma_x - \sigma_y)^2 + 4\tau_{xy}]^{\frac{1}{2}} I \quad (2)$$

Where $\sigma_{1,2}$ are principle stresses

Using Von- miss equation to know if the applied stresses in the plastic range as:

$$2\sigma_{yi}^2 = (\sigma_1 - \sigma_2)^2 + (\sigma_2 - \sigma_3)^2 + (\sigma_1 - \sigma_3)^2 \quad (3)$$

σ_{yi}*:* Yield stress*.*

Substitute result equation (2) into equation (3), get:

$$6\tau_{xy}^2 + C1 - C2 = 0 \quad (4)$$

Where C1, C2 are constant:

$C1=\sigma_x^2 + 2 * (0.5\sigma_x)^2 + 0.5 * (\sigma_x)^2$

$C2=2\sigma_y^2$

By evaluating the value of τ_{xy} from equation (4) and Substitute in equation (1) to get the maximum θ that can be applied in the experimental work.

Using tension and compression element to find principle stresses, for tension element case with torsional stress:

$$I_{11} = \sigma_{x1}+\sigma_{y1}+\sigma_{z1} \quad (5)$$

$$I_{21} = \sigma_{x1} * \sigma_{y1}+\sigma_{y1} * \sigma_{z1}+\sigma_{z1} * \sigma_{x1} - \tau_{xy1}^2 - \tau_{yz1}^2 - \tau_{zx1}^2 \quad (6)$$

$$I_{31} = \sigma_{x1} * \sigma_{y1} * \sigma_{z1} + 2 * \tau_{xy1}^2 * \tau_{yz1}^2 * \tau_{zx1}^2 - \sigma_{x1} * \tau_{yz1}^2 - \sigma_{y1} * \tau_{zx1}^2 - \sigma_{z1} * \tau_{xy1}^2 \quad (7)$$

$$\sigma^3 - I_{11}\sigma^2 - I_{21}\sigma - I_{31} = 0 \quad (8)$$

Then σ_{1t}, σ_{2t} *and* σ_{3t} Could be found by solving the roots of equation (8)

Same case for compression element to get on σ_{1c}, σ_{2c} *and* σ_{3c}

Now from two elements (tension-compression) mean stresses could be found, and substitute this stresses into octahedral stress equation for mean stress:

$$\sigma_{m.oct} = \frac{1}{\sqrt{2}} [(\sigma_{11m} - \sigma_{12m})^2 + (\sigma_{12m} - \sigma_{13m})^2 + (\sigma_{13m} - \sigma_{11m})^2]^{\frac{1}{2}} \quad (9)$$

Where $\sigma_{m.oct}$ is octahedral mean stress.

Too from two elements (tension- compression) get on amplitude stresses, and substitute this stress into octahedral stress equation for amplitude stress.

$$\sigma_{a.oct} = \frac{1}{\sqrt{2}}[(\sigma_{11a} - \sigma_{12a})^2 + (\sigma_{12a} - \sigma_{13a})^2 + (\sigma_{13a} - \sigma_{11a})^2]^{\frac{1}{2}} \text{ ......10}$$

Where $\sigma_{a.oct}$ is octahedral amplitude stress.

2.1 The suitable theoretical function to endurance limit stress for multiaxial fatigue

To find endurance limit stress for multiaxial fatigue it is found that three things must be considered:

1) The value of max shear stress resulting from the value of constant shear stress applied in non proportional loading and the phase angle between the normal stress resulting from cycling bending with the shear stress causes different orientation for principal stress and max shear stress in each cycle with the variation of the difference between octahedral amplitude and mean stress which effect on the crack propagation in multi axial and absent in uniaxial fatigue.

The cycling bending stress can be represented by the relation:

$$\sigma = \lambda\tau \sin \omega t \quad (11)$$

Where t= the period of one cycle in sec.

2) The ductility of the material causes a plastic region near the crack tip so that because the variation of the difference between the amplitude and mean stress in each cycle as mentioned above then the orientation of plastic zone will be different depend on the behavior of the material .

So that using criterion equation of Gerber for material of high ductility (as copper) which have greater plastic zone in multiaxial fatigue:

$$\frac{\sigma_{a.oct}}{\sigma_{e.m}} + (\frac{\sigma_{m.oct}}{\sigma_u})^2 = 1 \quad (12)$$

Where:

$\sigma_{e.m}$: Endurance limit stress for multiaxial fatigue.

while Using criterion equation for the Soderberg line for the material of medium ductility (as brass) which have approximately linear variation between the difference of octahedral mean and amplitude stress:

$$\frac{\sigma_{a.oct}}{\sigma_{e.m}} + \frac{\sigma_{m.oct}}{\sigma_u} = 1 \quad (13)$$

for steel , using criterion equation for the Soderberg line for the material , is depend on the percentage carbon in the composition which is for our material in this study it is recommended to use:

$$\frac{\sigma_{a.oct}}{\sigma_{e.m}} + \frac{\sigma_{m.oct}}{\sigma_{yi}} = 1 \quad (14)$$

The elastic range being given by Basquin's law and using endurance limit stress get:

$$2\sigma_{e.m} = (3.5\ \sigma_u) N_f^{-0.12} \qquad (15)$$

N_f: Number of cycle to failure.

3) The difference between octahedral amplitude strain and octahedral mean strain which varies in each cycle for multi axial fatigue must be calculated to give the effect of this variation on the N_f by using Basquins law and it verify the results of the stresses . It must be known that this variation is not pronounced in uniaxial fatigue.

The results repeating the above steps to the case of cyclic strain, get on octahedral equation for amplitude strain

$$\varepsilon_{a.oct} = \left(\frac{1}{1+v}\right)\frac{1}{\sqrt{2}} \left[(\varepsilon_{11a} - \varepsilon_{12a})^2 + (\varepsilon_{12a} - \varepsilon_{13a})^2 + (\varepsilon_{13a} - \varepsilon_{11a})^2\right]^{\frac{1}{2}} \qquad (16)$$

Where $\varepsilon_{a.oct}$ is octahedral amplitude strain.

And using Basquin's equation for octahedral amplitude strain:

$$2\varepsilon_{a.oct} = \left(\frac{3.5\ \sigma_u}{E}\right) N_f^{-0.12} \qquad (17)$$

3. The experimental work analysis

3.1 The new system added to the fatigue test

A rig consists of several parts as shown in **Fig.1**. It consists of electric motor, the specifications of electric motor were, power (1.5hp), voltage (220 volt), frequency (50Hz), and rotation velocity (3000rpm). The other part is to limit the amount of deflection (deformation part), this part is made using CNC wire cut machine, As well as the use of gearbox that have a reduction ratio (1:70), So that the process of twisting specimen at an angle (gearbox is used only in the case of bending with torsion) with connect the gearbox in the rear of the specimen as shown in **Fig.2**. A rig has three sensors, the first high accuracy proximity sensor (KFAPRN3514) calculates the number of cycles for electrical motor, it is placed against the outside of the shaft of the motor, the remaining sensors placed on a rig base on both sides of the crank**.** Can determine the amount of deflection using dial gauge with magnetic base are placed on a rig base. As well as the last part of Which can be controlling to know how many electric motor cycles meaning it contains data determines the number of cycles in the millions and other Parts of Millions, can be controlled through this to keep the number of cycles even after a power outage on a rig. A rig has been designed to be the base of the steel dimensions of (630mm) × (300mm), this rig is designed heavy weight in order to preserve stability at the shed large loads on the specimen, provided the base by four dampers to decrease the vibration generated from the electric motor rotation, as well as reduce the sound output of the motion. This device works on the principle cyclic strain, because the deflection remains constant.

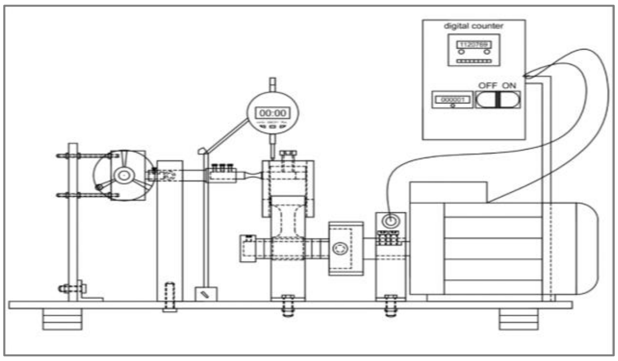

Figure 1 Auto CAD planner rig system

Figure 2 Rig system

3.2 Properties of metals specimens

It have been shown that the important points in determining the fatigue life of metals is the ductility which causes the fatigue crack growth to by very slow and bounded the region around the crack. This can be achieved by taking in to consideration the chemical composition, the mechanical properties and hardness number of each metal as shown in **Tables 1, 2, 3 and 4**.

Table 1 Chemical compositions and mechanical properties for (L690M) steel

C	Cr	Mo	Si	Al	Cu	V	Fe
0.012	4.97	2.74	0.29	0.3	0.04	1.32	Rem

Yield S. (σ_y) Mpa	Ultimate S. (σ_u) Mpa	Young Modulus (E) Gpa	Hardness HV
882	910	200	314

Table 2 Chemical compositions and mechanical properties for (C26800) brass

Cu	Zn	Cr	Si	Al	Mn	Ni	Fe
64.92	34.98	0.01	0.01	0.02	0.01	0.01	0.03

Yield S. (σ_y) Mpa	Ultimate S. (σ_u) Mpa	Young Modulus (E) Gpa	Hardness HV
420	552	110	172

Table 3 Chemical compositions and mechanical properties for Copper

Fe	Cr	Mo	Si	Ni	Ti	V	Cu
0.774	0.11	0.001	0.062	0.01	0.04	0.001	Rem
Yield S. (σ_y) Mpa		Ultimate S. (σ_u) Mpa		Young Modulus (E) Gpa		Hardness HV	
292		302		100		--	

Table 4 Chemical compositions and mechanical properties for (2117-T4) Aluminum

Fe	Cr	Mo	Si	Ni	Cu	V	Al
0.979	0.05	0.11	0.01	0.05	0.03	0.01	Rem
Yield S. (σ_y) Mpa		Ultimate S. (σ_u) Mpa		Young Modulus (E) Gpa		Poissons ratio (υ)	
173		303		69		0.33	

3.3 Fatigue Specimen's Preparation

The shape and dimensions of the required fatigue test specimens, which is suitable for **ASTM** standard rotating fatigue test machine is shown in **Fig.3** & **Fig.4**. The fatigue specimens manufactured for all tests (bending and bending with torsion) through the CNC lathe machine (STAR CHIP 450), So it has been a major program and sub-program is composed of 24 step by feed 0.3 and speed of rotation of the machine in 1200 rpm, then the sub-program for finishing surface consist of two steps by feed 0.01 and the speed of the machine in 1500 rpm, the final surface of the specimen is very satin and does not contain any deformation.

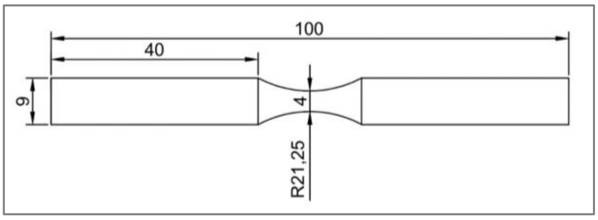

Figure 3 Dimension of fatigue test specimen (all dim. in mm)

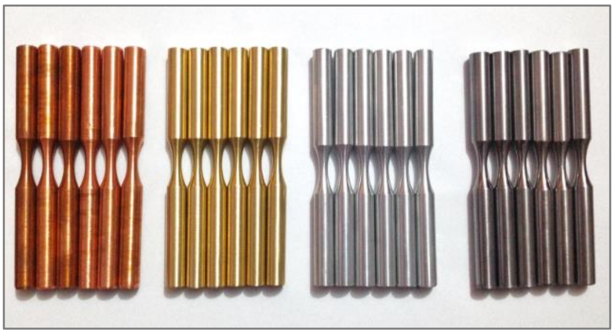

Figure 4 Shape of Multi axial fatigue test specimens

4. Result and discussion

4.1 Uniaxial and multiaxial fatigue test

Completed test reversed bending firstly and bending with torsion on several specimen on metals listed above has been verify the validity of the results reversed bending case for each metal by comparing them with standard tables and equations developed in MATLAB program. It turns out that the form of the fracture of the specimen in the test case reversed bending is a horizontal fracture surface plane as shown in **Fig.5-A** either in a test case combined bending with torsion appeared in the form of the fracture surface sloping at an angle as a result of specimen exposure to twisting as shown in **Fig.5-B**, this conforms with the Mohr circle theory**.**

(A) (B)

Figure 5 A-Surface fracture for (Reversed bending) fatigue, B-Surface fracture for (bending with torsion) fatigue

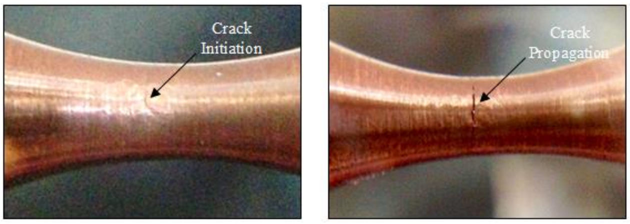

(A) (B)

Figure 6 A- Crack initiation in case (Reversed bending fatigue), B- Crack evolution in case (Reversed bending fatigue)

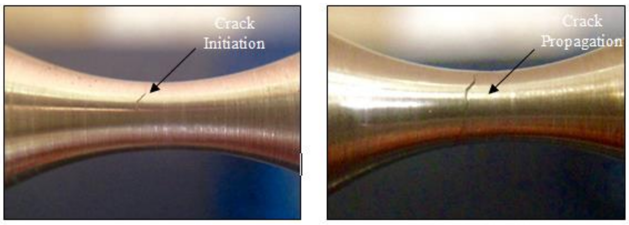

(A) (B)

Figure 7 A- Crack initiation in case (Bending with torsion fatigue), B- Crack evolution in case (Bending with torsion fatigue)

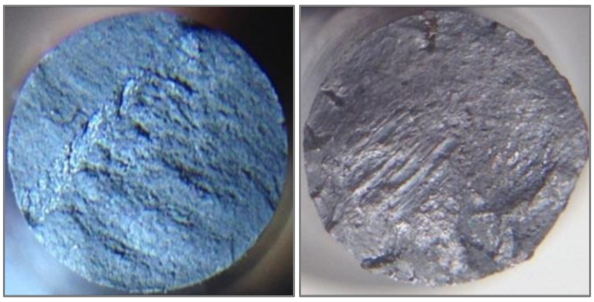

(A) (B)

Figure 8 (L690M) steel A-Surface fracture for (Reversed bending) fatigue, B-Surface fracture for (bending with torsion) fatigue

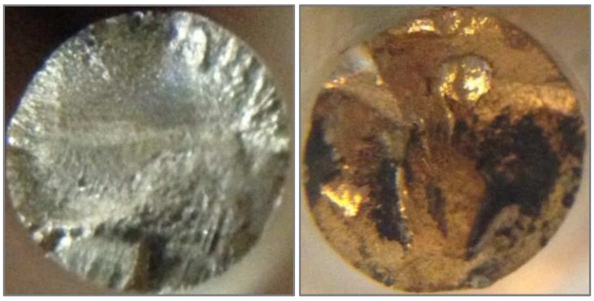

(A) (B)

Figure 9 (C26800) brass A-Surface fracture for (Reversed bending) fatigue, B-Surface fracture for (bending with torsion) fatigue

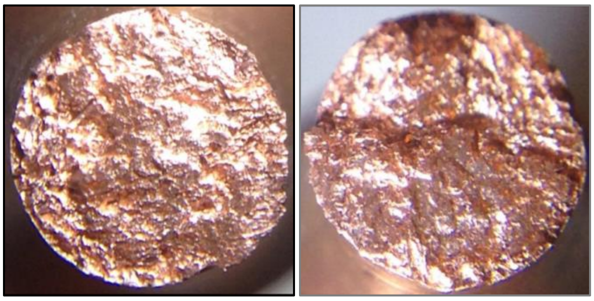

(A) (B)

Figure 10 Copper A-Surface fracture for (Reversed bending) fatigue, B-Surface fracture for (bending with torsion) fatigue

(A) (B)

Figure 11 (2117-T4) Aluminum A-Surface fracture for (Reversed bending) fatigue, B-Surface fracture for (bending with torsion) fatigue

Table 5 Reversed bending and multiaxial fatigue test for (L690M) steel

Reversed bending test				Multiaxial fatigue test					
N.	σ_b(Mpa)	ε	N_f	N.	ε	τ(Mpa)	λ	θ°	N_f
1	600	0.00299	1200	1	0.00299	51.9	0.086	1	1000
2	550	0.00274	7900	2	0.00274	51.9	0.094	1	4500
3	432	0.00215	55000	3	0.00215	51.9	0.12	1	51010
4	360	0.00179	120000	4	0.00179	51.9	0.144	1	80600
5	300	0.00149	1600000	5	0.00149	51.9	0.173	1	900100

Table 6 Reversed bending and multiaxial fatigue test for (C26800) brass

Reversed bending test				Multiaxial fatigue test					
N.	σ_b(Mpa)	ε	N_f	N.	ε	τ(Mpa)	λ	θ°	N_f
1	375	0.003408	1200	1	0.003408	47.9	0.127	2	1017
2	307	0.00279	10072	2	0.00279	47.9	0.156	2	6500
3	254	0.002308	96000	3	0.002308	47.9	0.188	2	84011
4	210	0.001908	700000	4	0.001908	47.9	0.228	2	401196
5	191	0.001735	900034	5	0.001735	47.9	0.25	2	580090
6	180	0.001636	1320000	6	0.001636	47.9	0.266	2	1000121

Table 7 Reversed bending and multiaxial fatigue test for Copper

Reversed bending test				Multiaxial fatigue test					
N.	σ_b(Mpa)	ε	N_f	N.	ε	τ(Mpa)	λ	θ°	N_f
1	220	0.0022	1100	1	0.0022	54.7	0.248	2	1003
2	150	0.0015	48018	2	0.0015	54.7	0.364	2	12018
3	117	0.00117	320012	3	0.00117	54.7	0.467	2	90011
4	100	0.001	1023090	4	0.001	54.7	0.547	2	821009

Table 8 Reversed bending and multiaxial fatigue test for (2117-T4) Aluminum

Reversed bending test				Multiaxial fatigue test					
N.	σ_b(Mpa)	ε	N_f	N.	ε	τ(Mpa)	λ	θ°	N_f
1	195	0.00282	2006	1	0.00282	34.9	0.178	2	1276
2	152	0.0022	41009	2	0.0022	34.9	0.229	2	10300
3	130	0.00188	100187	3	0.00188	34.9	0.268	2	42015
4	104	0.0015	680000	4	0.0015	34.9	0.335	2	140012
5	93	0.00134	1325060	5	0.00134	34.9	0.375	2	810117

4.2 Cyclic strain in uniaxial and multiaxial fatigue

4.2.1 For (L690M) steel

All the results are shown in **Table 5**, and the resulting empirical equations as Eq. (18) for reversed bending fatigue test and Eq. (19) for multiaxial bending with torsion fatigue test as shown in **Fig. 12 & Fig. 13**:

$$\varepsilon=0.0065(N_f)^{-0.104} \quad (18)$$
$$\varepsilon=0.0065(N_f)^{-0.108} \quad [\tau=51.9\ \text{Mpa}] \quad (19)$$

4.2.2 For (C26800) brass

All the results are shown in **Table 6**, and the resulting empirical equations as Eq. (20) for reversed bending fatigue test and Eq. (21) for multiaxial bending with torsion fatigue test as shown in **Fig. 14 & Fig. 15**:

$$\varepsilon=0.0071(N_f)^{-0.101} \quad (20)$$

$$\varepsilon=0.007(N_f)^{-0.103} \quad [\tau=47.9\ \text{Mpa}] \quad (21)$$

4.2.3 For Copper

All the results are shown in **Table 7**, and the resulting empirical equations as Eq. (22) for reversed bending fatigue test and Eq. (23) for multiaxial bending with torsion fatigue test as shown in **Fig. 16 & Fig. 17**:

$$\varepsilon=0.005(N_f)^{-0.115} \quad (22)$$
$$\varepsilon=0.0048(N_f)^{-0.119} \quad [\tau=54.7\ \text{Mpa}] \quad (23)$$

4.2.4 For (2117-T4) Aluminum

All the results are shown in **Table 8**, and the resulting empirical equations as Eq. (24) for reversed bending fatigue test and Eq. (25) for multiaxial bending with torsion fatigue test as shown in **Fig. 18 & Fig. 19**:

$$\varepsilon=0.007(N_f)^{-0.115} \quad (24)$$

$$\varepsilon=0.0066(N_f)^{-0.12} \quad [\tau=51.9\ \text{Mpa}] \quad (25)$$

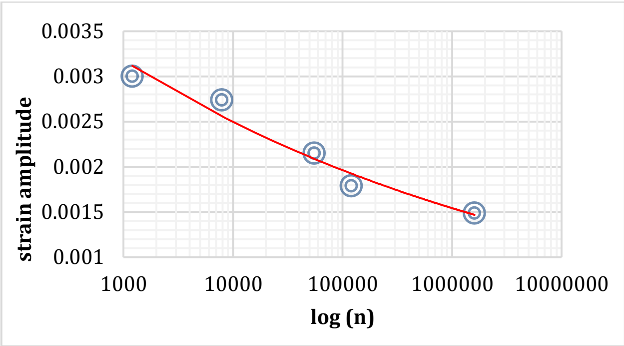

Figure 12. Experimental cyclic strain reversed bending fatigue test for (L690M) steel

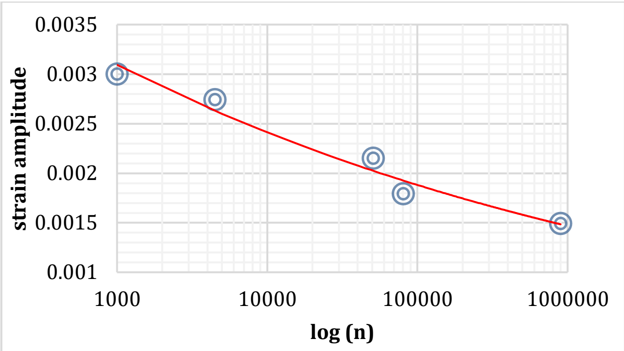

Figure 13 Experimental cyclic strain bending with torsion fatigue test for (L690M) steel

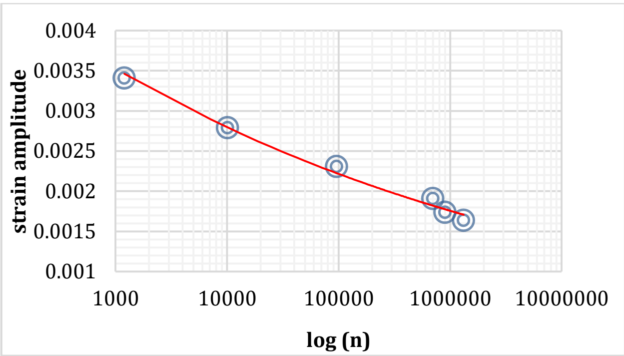

Figure 14 Experimental cyclic strain reversed bending fatigue test for (C26800) brass

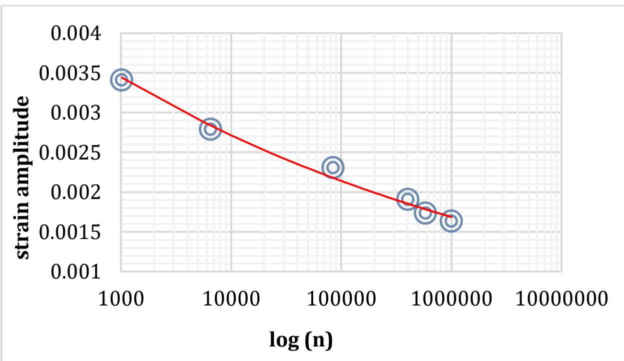

Figure 15 Experimental cyclic strain bending with torsion fatigue test for (C26800) brass

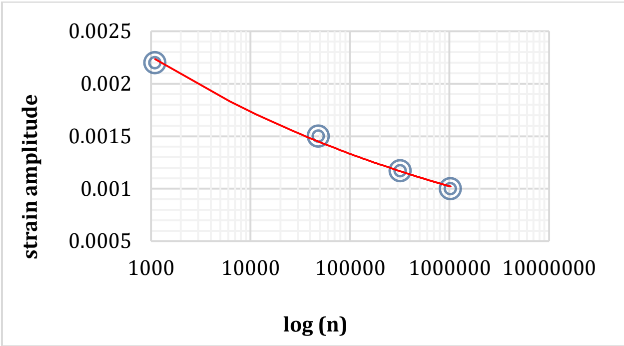

Figure 16 Experimental cyclic strain reversed bending fatigue test for Copper

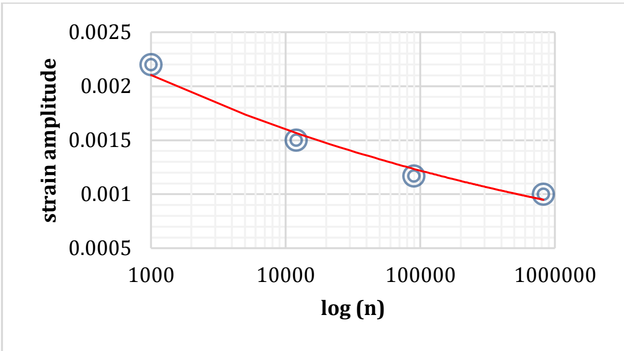

Figure 17 Experimental cyclic strain bending with torsion fatigue test for Copper

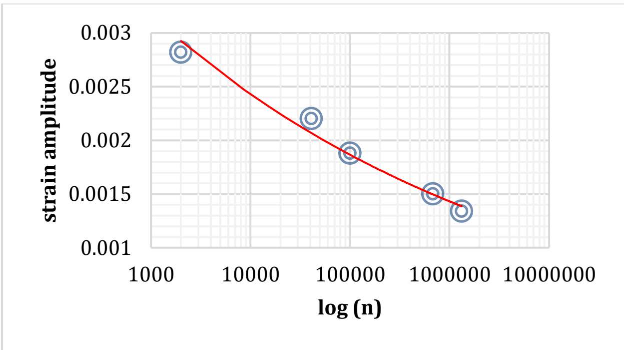

Figure 18 Experimental cyclic strain reversed bending fatigue test for (2117-T4) Aluminum

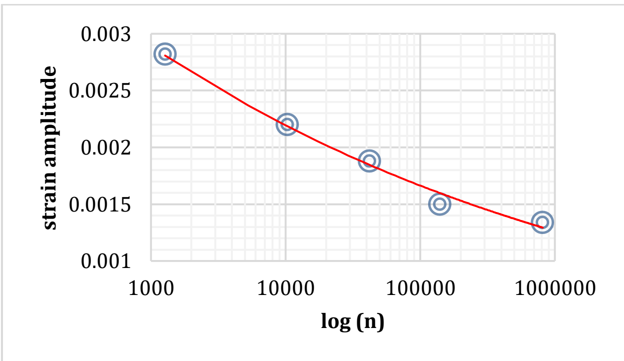

Figure 19 Experimental cyclic strain bending with torsion fatigue test for (2117-T4) Aluminum

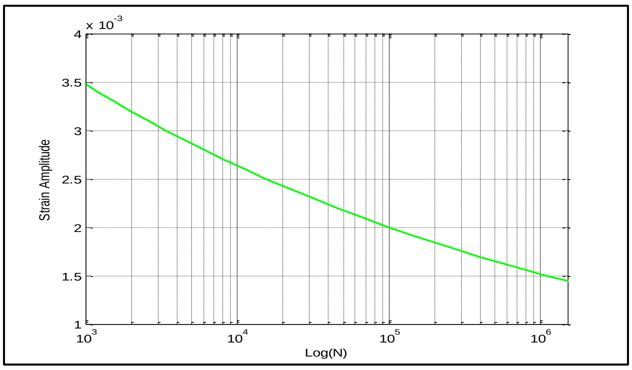

Figure 20 Theoretical cyclic strain reversed bending fatigue test for (L690M) steel

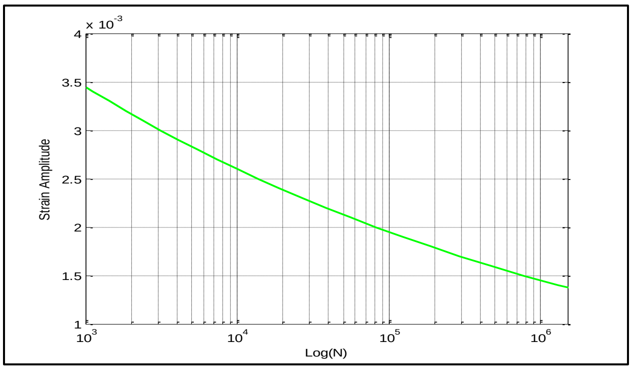

Figure 21 Theoretical cyclic strain multiaxial bending with torsion fatigue test for (L690M) steel

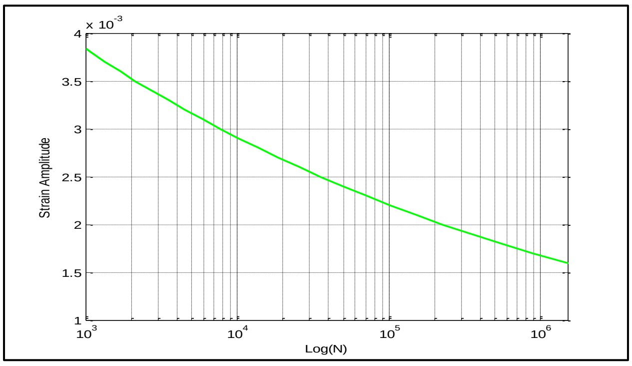

Figure 22 Theoretical cyclic strain reversed bending fatigue test for C26800 brass

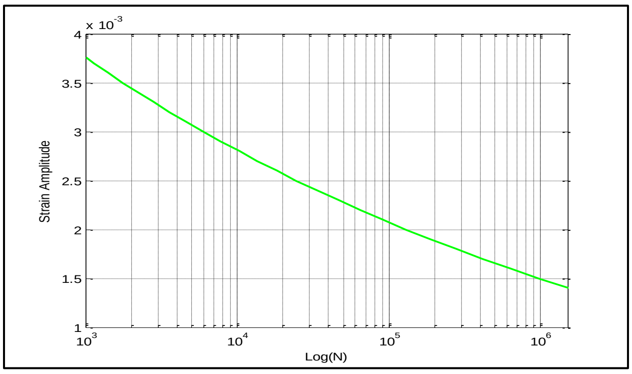

Figure 23 Theoretical cyclic strain multiaxial bending with torsion fatigue test for C26800 brass

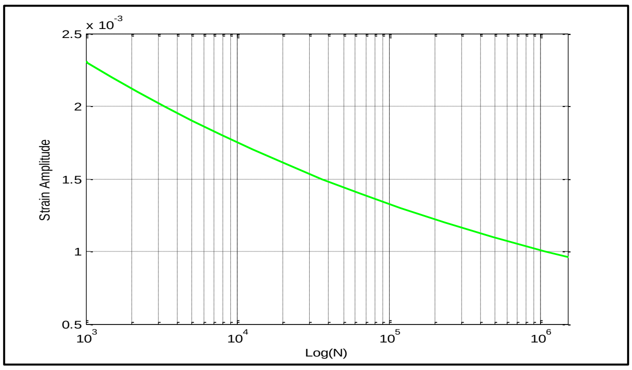

Figure 24 Theoretical cyclic strain reversed bending fatigue test for copper

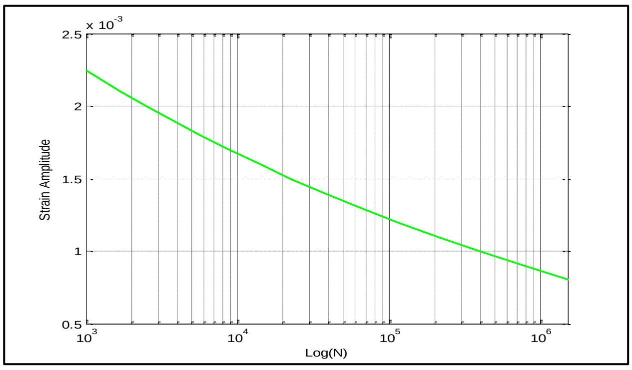

Figure 25 Theoretical cyclic strain multiaxial bending with torsion fatigue test for Copper

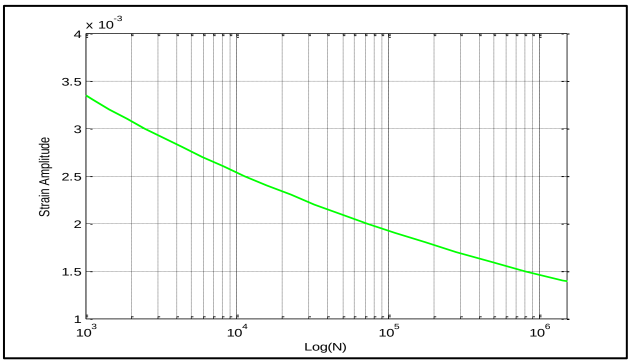

Figure 26 Theoretical cyclic strain reversed bending fatigue test for 2117-T4 Aluminum

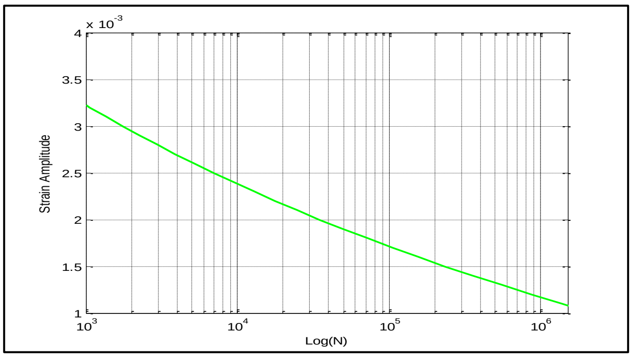

Figure 27 Theoretical cyclic strain multiaxial bending with torsion fatigue test for 2117-T4 Aluminum

Conclusion

1) In the test multiaxial combined bending with torsion fatigue is life estimation less than what is in the test case reversed bending with constancy amplitude stresses and add shear stress in the test case multiaxial.

2) After staying ratio ($\lambda = \tau / \sigma_a$) fixed for all metal, showing that copper is the safer in the test case multiaxial and 2117-T4 aluminum less safe, then C26800 brass and L690M steel is more dangerous.

3) The configuration of the fracture surface in the standard specimen in the case of reversed bending horizontal plane, either in the case of specimen exposed to multiaxial fatigue (bending with torsion) shall breakage italic angle as a result of twisting, and this corresponds to the theory Mohr circle, and this is what is happening since the beginning of the crack and even fracture

4) Ductility of metals are considered stubborn metals in fatigue testing, where area of crack initiation after the fracture of metals (copper, 2117-T4 aluminum) greater than it is in metals, the most hardness (L690M steel, C26800 brass).

References

Ali Fatemi, Nima, S., 2011 *Multiaxial Fatigue: An Overview and Some Approximation Models for Life Estimation,* International Journal of Fatigue 33–948–958 University of Toledo, USA.

Bernasconi, S. Foletti, I. V., 2005, *Multiaxial Fatigue Test under Combined Torsion and Axial Load with Different Frequencies*, Milano, Italy.

Zbigniew, M., Dariusz, R., Ewald, M., 2007, *Fatigue Lives of 18G2A and 10HNAP Steels under Variable Amplitude and Random Non-Proportional Bending with Torsion Loading,* Opole University of Technology, Poland.

Xiao, Y. L., Tie, X. S., Yi, Z., Mei, N. Y., 2015, *A Multiaxial High-Cycle Fatigue Life Evaluation Model For Notched Structural Components*, University of China, Taiyuan.

K. J. Miller and M. W. Brown, 1999 *Multiaxial fatigue*, University of Sheffield.

Nomenclature

λ : stress amplitude ratio (λ = τ /σ_a).
τ : reversed torsion fatigue strength, Mpa.
σ_a: reversed bending fatigue strength, Mpa.
M: moment, N.m.
I: moment of inertia, mm^4 .
F: force, N.
L: length, mm.
d: diameter, mm.
E: models of elasticity, Mpa.
ΔL: deflection, mm.
r: radius of specimen, mm.
ε: strain amplitude.
N_f: number of cycle to failure.